Limnol. Oceanogr., 53(6), 2008, 000–000

Evidence for the inherent unsteadiness of a river plume: Satellite observations of the Niagara River discharge

A. R. Horner-Devine
Civil and Environmental Engineering, University of Washington, Seattle, Washington 98195

D. A. Fong and S. G. Monismith
Civil and Environmental Engineering, Stanford University, Stanford, California 94305

Abstract

1

We present satellite data from the Niagara River plume showing that a large eddy, or bulge, forms and grows in the plume near the mouth of the river. The plume consists of a semicircular bulge region immediately offshore of the mouth and a narrow current that propagates east along the shoreline. During the low-wind period from 27 to 29 May 1999, the width of the bulge more than doubled and the current width increased only slightly. Approximately one-third of the Niagara River water accumulated in the bulge near the mouth during this period, implying that the transport rate in the shore-parallel current was reduced to two-thirds of the river discharge rate. The effective radius and the growth rate of the bulge computed from the satellite images was in good agreement with previous laboratory results and a numerical model of the Niagara River plume. This is the first field evidence of the unsteadiness of the bulge.

When buoyant water is discharged from a large-scale river into an otherwise quiescent basin, it is turned to the right (in the Northern Hemisphere) by the Coriolis force and eventually forms a current along the right-hand coast. This is observed in numerous river plumes (Masse and Murthy 1992; Hickey et al. 1998) and in large ocean inflows (Lanoix 1974). Traditionally, models have assumed that the coastal current transports all of the river water away from the mouth and, therefore, that the plume is in steady state. Idealized numerical, laboratory, and analytical studies, however, predict that a growing anticyclonic eddy, or bulge, forms at the river mouth (Nof and Pichevin 2001; Fong and Geyer 2002; Horner-Devine et al. 2006), contradicting the steady-state assumption. In these models, the freshwater transport in the coastal current is lower than the river discharge, implying that some of the river water returns to the bulge instead of flowing down the coast. Thus, the alongshore transport and retention of the plume water near the mouth differ significantly in an unsteady plume in comparison with a steady-state plume.

The reduced flow in the coastal current may have important consequences for transport of sediments, nutrients, and contaminants typically carried by river water since the coastal current is the primary means of removing river water from the vicinity of the river mouth.

Although field evidence of a bulge has been documented in some river plumes, no study has confirmed the growth, and hence, unsteadiness, of the bulge in nature. Determining whether or not the bulge is indeed unsteady is difficult with in situ data since synoptic measurements of a feature of this size are challenging. Additionally, variability due to winds and tides may obscure the relatively smaller change in size associated with bulge unsteadiness. In this paper we use satellite data to present evidence of a growing bulge in the Niagara River plume in Lake Ontario and compare the observed bulge growth with idealized laboratory and numerical modeling experiments. The Niagara plume is a convenient choice for testing the unsteady behavior observed in idealized models since tides are minimal in Lake Ontario. In addition, we select a time period when the winds are relatively low.

Acknowledgments

A.H.-D. thanks K. Arrigo for his introduction to remote sensing. We also thank Jonathan Warrick and one anonymous reviewer for their careful reading of the manuscript.

We are grateful for support from the National Science Foundation grant OCE-0118029.

Background

In an analytical study, Pichevin and Nof (1997) consider a control volume drawn around the mouth of a buoyant ocean inflow. They show that no force exists to balance the flow force imparted on the control volume by the water leaving in the coastal current. Thus, the traditional model of a steady-state, buoyant plume cannot exist. They refer to this as the momentum imbalance paradox. In a subsequent analytical study, Nof and Pichevin (2001) show that bulge growth results in a force in the opposite direction to the coastal current flow force and, thus, the momentum imbalance paradox is resolved when the plume is not constrained to be steady.

Numerical and laboratory models also produce a growing bulge. This feature is typically more pronounced when the model configuration consists of a steep or vertical coastal wall (Garvine 2001) in combination with relatively high stratification, resulting in a "surface-advected" river plume (Yankovsky and Chapman 1997). A numerical study by Fong and Geyer (2002) finds that between 25% and 75% of the river water accumulates near the river mouth instead of moving downstream in the coastal current as has traditionally been assumed. Using a laboratory river plume model consisting of a constant buoyant inflow on a rotating tank,

Horner-Devine et al. (2006) show that a bulge forms and grows, consistent with Fong and Geyer (2002) and the laboratory experiments of Avicola and Huq (2003). The data from both laboratory studies show that the bulge depth scales with $h_p = (2Qf/g')^{1/2}$ and the radius scales with the internal Rossby radius $L_b = \left(2Qg'/f^3\right)^{1/4}$. Both the depth and the radius increase over the course of these experiments.

Despite evidence from numerical, laboratory, and analytical models that the bulge grows in time, no field studies have confirmed such a phenomenon. The presence of anticyclonic eddies near river mouths has been documented in field studies of the Niagara River plume (Masse and Murthy 1992), the Columbia River plume (Hickey et al. 1998; Horner-Devine 2008), and the Hudson River plume (Chant et al. 2008). None of these studies, however, reports sampling the structure of the entire plume in such a fashion that the growth of the bulge could be measured.

Satellite remote sensing offers a solution to this problem since synoptic images of a specific region of interest are typically obtained once or twice each day. Satellite surface color data from the sea-viewing wide field-of-view (SeaWIFS) sensor platform have been used to observe several river plumes such as the Mississippi (Salisbury et al. 2004), the Columbia (Thomas and Weatherbee 2006), and a series of coastal California plumes (Mertes and Warrick 2001; Warrick and Fong 2004). In general, the normalized water-leaving radiance, nLw, at higher wavelengths (555 nm or 667 nm) is correlated with the plume location (Salisbury et al. 2004; Thomas and Weatherbee 2006), as these wavelengths are most sensitive to suspended sediment in the water column. Despite the ease of use of the satellite data, considerable caution must be used in interpreting surface color fields for the purposes of plume detection. This is discussed in detail in the methods section.

Study area

The Niagara River runs through a highly industrialized region of northern New York state between Lake Erie and Lake Ontario (Fig. 1). It has been the subject of considerable study during the past decades as it has historically carried high concentrations of toxic industrial chemicals such as polychlorinated biphenyls (PCB)s, dichlorodiphenyltrichloroethane, Mirex, and dioxins into Lake Ontario (U.S. EPA and NYSDEC 1998). Efforts to reduce the source of chemicals to the river have begun to show signs of success (U.S. EPA and NYSDEC 1998). Since the river is the source of many contaminants entering the lake, and the fate of the contaminants is closely linked to the plume circulation, considerable effort has been taken to better understand the dynamics of the Niagara discharge (Murthy 1996). A comprehensive set of experiments from 1983 to 1985 has been used to map the temperature and velocity fields of the plume (Masse and Murthy 1990, 1992) and compare them with the observed distribution of contaminated bottom sediments (Thomas 1983; Murthy 1996). Masse and Murthy (1990) describe three distinct regions of the plume. Within 5 km of the mouth the lake is shallow, the plume is well mixed to the bottom, and the dynamics are influenced primarily by the momentum of the river discharge and the bottom stress. The lake deepens rapidly beyond this near-field region and the plume separates from the bottom, entering a second region where advection, Coriolis force, wind stress, and buoyancy are all important. Still farther from the mouth, the influence of the river momentum diminishes and the dynamics are set by Coriolis force, buoyancy, and wind stress. In a subsequent analysis, Masse and Murthy (1992) use data from a mooring array and ship-tracked drifters to estimate the magnitude of each term in the momentum balance. Although the results of this work generally support the description of the plume in Masse and Murthy (1990), their estimates suggest that local wind stress is only a second-order term, except during high winds. They suggest instead that winds may be most important in setting up a persistent cyclonic current along the south shore of the lake.

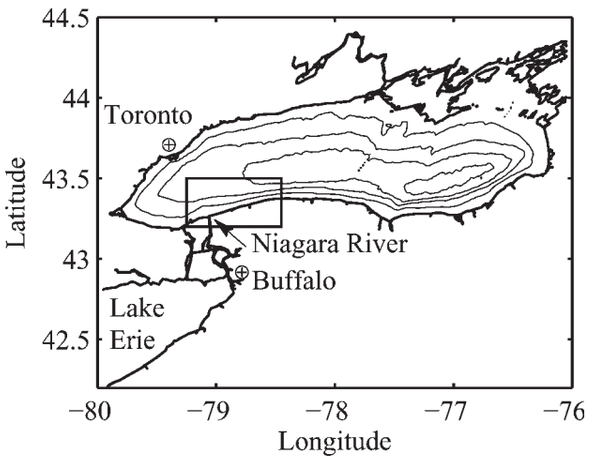

Fig. 1. Bathymetric map of Lake Ontario. Thin lines represent 50-m contour lines. The Niagara River plume region is indicated by the rectangle. Bathymetric and coastline data are from the National Oceanic and Atmospheric Administration (NOAA) National Geophysical Data Center.

Overall, Masse and Murthy (1990, 1992) describe a plume that is very similar in structure to the plume observed in laboratory, numerical, and analytical model studies. The river water executes a turn to the right as it exits the river mouth, forming a broad semicircular turning region with a width greater than the internal Rossby radius (e.g., Garvine 1987). Masse and Murthy (1990, 1992) report a value for the internal Rossby radius of 2–3 km during summer months. Downstream of the bulge, in the sense of Kelvin wave propagation, the plume water forms a current parallel to the shoreline, with a width approximately equal to the internal Rossby radius. This structure is clear in the visible band image and contoured lake surface temperature plot in Masse and Murthy (1992, their figs. 2b and 3, respectively). The qualitative agreement between the observed plume structure and laboratory and numerical models suggests that the Niagara plume may also display the unsteady bulge behavior predicted by those models. Indeed, Murthy (1996) presents data on the basis of tracers released in the river mouth that make an anticyclonic loop east of the mouth with diameter 5–7 km.

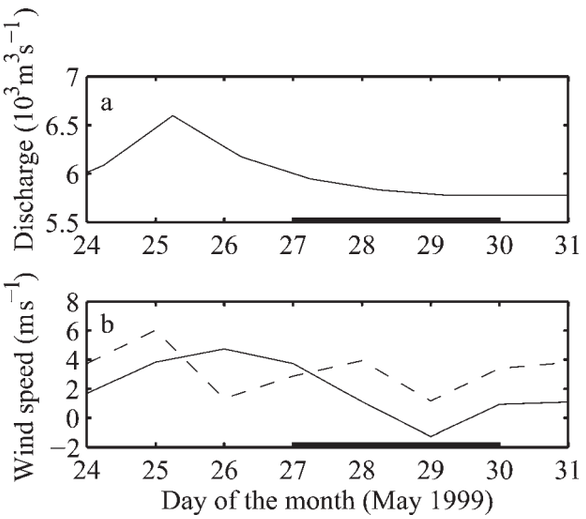

Fig. 2. Niagara River discharge and local wind, 24–31 May 1999. (a) Discharge, measured at the head of the river, shifted by 18 h to account for the propagation time in the river. (b) Wind speed measured at St. Catherines airport. Solid line: alongshore wind; dashed line: cross-shore wind. In panels a and b the solid bar of the time axis corresponds to the study period.

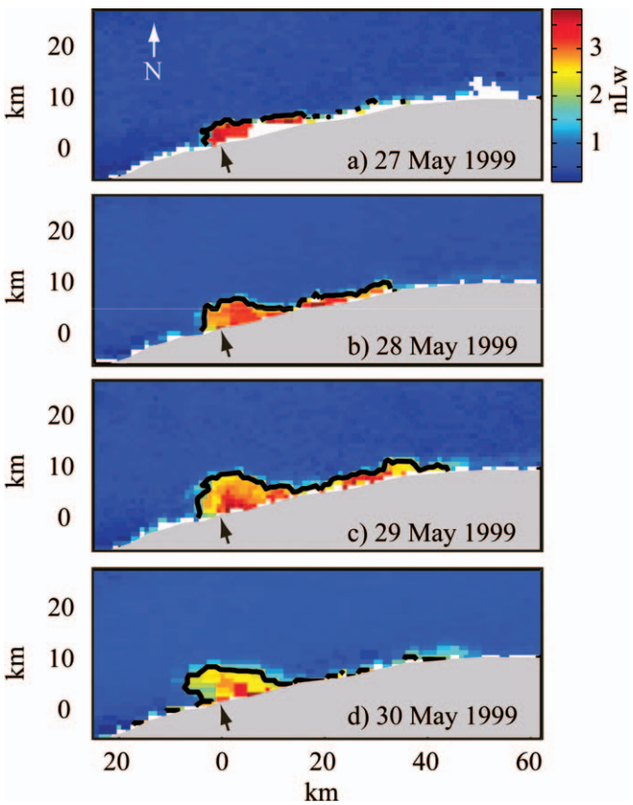

Fig. 3. Normalized water-leaving radiance showing the Niagara River plume on (a) 27 May 1999, (b) 28 May 1999, (c) 29 May 1999, and (d) 30 May 1999. The color corresponds to normalized water-leaving radiance (nLw) in the 555-nm band in units of mW cm^{-2} μm^{-1} sr^{-1}. The black contour indicates the threshold chosen to represent the edge of the plume and the Niagara River mouth is indicated by the black arrow. White cells near the shoreline are bad data.

Methods

In this study we use satellite data to examine the Niagara River plume during the period 27 to 30 May 1999. The primary data considered are from the SeaWIFS satellite sensor, which has 1.1-km spatial resolution and orbits the earth once each day.

Since Lake Erie is considerably shallower than Lake Ontario, it is typically 3–4°C warmer in the spring and fall (Masse and Murthy 1992) and thus Niagara River water is about 0.8 kg m^{-3} lighter than ambient Lake Ontario water. The Niagara River was chosen because it is approximately perpendicular to the shoreline, empties into a deep basin, and is large enough for the earth's rotation to be relatively important. According to temperature transects from field studies (Masse and Murthy 1992), the Niagara plume is detached from the lake bottom over much of its width in the spring and fall.

The criteria for choosing the study period were that four consecutive days were cloud free and that there was little unsteady forcing. Plume unsteadiness may result from significant wind stress or fluctuations in the river discharge. We examined all SeaWIFS images of the Lake Ontario region during the 3 yr from 1997 to 1999 and chose 27 to 30 May 1999 on the basis of the above criteria.

The river discharge is monitored at the head of the river in Lake Erie. In Fig. 2a the discharge is plotted with the time axis shifted by 18 h to account for the propagation time in the river (Atkinson et al. 1994). The average discharge was approximately 5900 m^3 s^{-1} and it decreased by 4% during the study period. The discharge peaked 2 d before the study period; however, the response time of plumes is typically on the order of 1 d, and thus our data are not expected to reflect this peak. The satellite images are consistent with this assumption. We obtained a wind record from the nearby St. Catherines airport and calculated average alongshore and across-shore winds for each day (Fig. 2b). The alongshore wind, which exerts a stronger influence over the cross-shore dynamics of the plume (Chao 1988), is moderate and downwelling favorable on the first day of the study period, 27 May. It decreases slightly on 28 May, is light on 29 May, and increases again slightly on 30 May.

The nLw at 555 nm is presented for all 4 d in Fig. 3 for the Niagara River plume region shown in Fig. 1. Several assumptions must be made for the surface color anomaly in Fig. 3a–d to be used with confidence to delineate the river plume. First, the color anomaly is assumed to correspond to suspended sediment in the water column. The 555-nm wavelength is in the green region of the color spectrum and is typically scattered by sediments and, to a lesser degree, biological matter such as plankton. We plotted images of the chlorophyll product (not shown), which did not display a strong signal, and concluded that the images in Fig. 3 represent sediments. This is consistent with several previous studies that use the 555-nm band to delineate plume waters

on the basis of suspended sediments in satellite images (Mertes and Warrick 2001; Thomas and Weatherbee, 2006). In the present data, nLw at higher wavelengths also showed similar structure in the region of the plume. However, we concentrate on the 555-nm band for simplicity.

The second assumption is that the plume has a higher suspended sediment concentration than the ambient lake water and that the river is the dominant source of sediment to the plume. Previous studies of the Niagara River estimate the river contribution of silt and clay-sized materials to Lake Ontario as about 4.56 billion kg yr^{-1} or 50% of the total (Kemp and Harper 1976). This suggests that the river is the primary sediment contribution in the region being considered. Furthermore, the Niagara sediments are fine and, thus, expected to settle out of the plume very slowly.

A fall velocity estimate can be used in conjunction with scales for the plume length and propagation speed to determine the expected scale of the sediment signature. On the basis of Stokes' law, a reasonable settling velocity for a fine silt particle with diameter 5×10^{-6} m is $u_{\text{fall}} = 2 \times 10^{-4}$ m s^{-1}. Although a significant fraction of the sediment will flocculate and fall out of the plume more rapidly, the disaggregated fraction will persist downstream and result in a longer-lived surface signature. The approximate scales for the plume depth and velocity are h_p and $u_p = (2Qfg')^{1/4}$ (Lentz and Helfrich 2002; Horner-Devine et al. 2006). For the Niagara River during the study period, $g' = g\Delta\rho/\rho = 0.006$ m s^{-2}, $f = 1.0 \times 10^{-4}$ s^{-1}, and, thus, $h_p = 13.8$ m and $u_p = 0.3$ m s^{-1}. The velocity estimate is likely to be low in the region near the river mouth and high in the buoyant shore-trapped current east of the mouth. On the basis of the plume depth and speed, sediment particles should be retained in the plume layer for a distance $L_s = h_p u_p u_{\text{fall}}^{-1} = 18$ km. Thus, fine sediments will be retained in the plume beyond the bulge region. The presence of a westerly wind, favoring downwelling, is expected to increase the alongshore surface current. During downwelling periods, Geyer et al. (2000) found that fine sediment is carried more than 60 km north of the mouth in the Eel River plume, California. Although this result is also likely to be a function of the low inflow angle of the Eel plume, it suggests that the low downwelling wind during the study period considered in the present study is likely to increase L_s. Finally, the role of sediment resuspension in the near-shore region must also be considered. Since the plume depth is on the order of the local water depth, it is likely that sediment is suspended and entrained into the plume as the buoyant shore-trapped current travels to the east. This may provide an additional source of sediment to the current that allows it to be visible farther from the river mouth. In the near-field region, near the center of the bulge, the plume is in contact with the bottom because of the shallow bar and is known to resuspend sediment. However, since the wind stress decreases over the first 3 d, resuspension of sediment by the wind cannot explain the increase in plume size. Therefore, the surface color anomaly is considered to be representative of the location of the plume.

As further confirmation that the surface color data can be used to determine the extent of the plume, the sea surface temperature for 29 May 1999, the third day of the study period, is shown in Fig. 4. Because of limitations in data availability and cloud cover, this is the only thermal image available. Although local heating often dominates sea surface temperature images, recent work suggests that stratified plumes can be detected in these images because of their anomalous heating patterns (de Boer et al. 2008). The data in Fig. 4 show a region of higher surface temperature that corresponds very closely with the surface color anomaly from the same day (Fig. 3c). In Fig. 4 the temperature difference between the plume water and the ambient lake water is approximately 6°C.

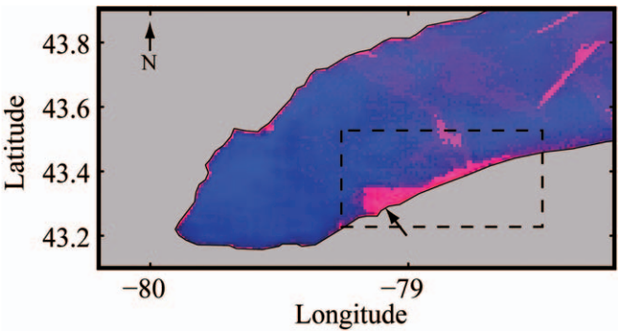

Fig. 4. Surface temperature at 18:30 h coordinated universal time on 29 May 1999 from advanced very-high-resolution radiometer sensor. The plume and ambient lake temperatures are approximately 12°C and 6°C. The diffuse regions of higher temperature to the north and east of the plume are most likely the result of thin cloud cover. The rectangle shows the approximate boundary of the SeaWIFS images in Fig. 3 and the arrow shows the location of the river mouth.

Results

On 27 May the plume is slightly wider near the river mouth than downstream along the shore, although no bulge is evident. The bulge forms and grows on 28 and 29 May and maintains its size on 30 May. The plume appears more diffuse on 30 May. This may also be a result of lower resolution on 30 May due to the fact that the zenith angle of the satellite was much lower than on the first 3 d. The coastal current width does not appear to increase in the same manner as the bulge; instead, it maintains a relatively constant width.

The bulge and coastal current structure of the plume on 28 to 30 May 1999 appears in satellite images from many other days (not shown) and is very similar to the density structure in numerical and laboratory studies (Fong and Geyer 2002; Horner-Devine et al. 2006). In addition, it is consistent, both in shape and horizontal extent, with the surface temperature distribution found in field studies of the Niagara River plume (Masse and Murthy 1992; Fig. 6). We conclude, therefore, that the plume structure in Fig. 3a–d is representative of the density field of the plume.

To quantify the growth of the bulge, we measured the area A_b occupied by the bulge on each day. This was done by determining the number of pixels within a prescribed area at the river mouth whose intensity exceeded a threshold value. The contour value chosen to represent the approximate edge of the plume is shown in Fig. 3a–d.

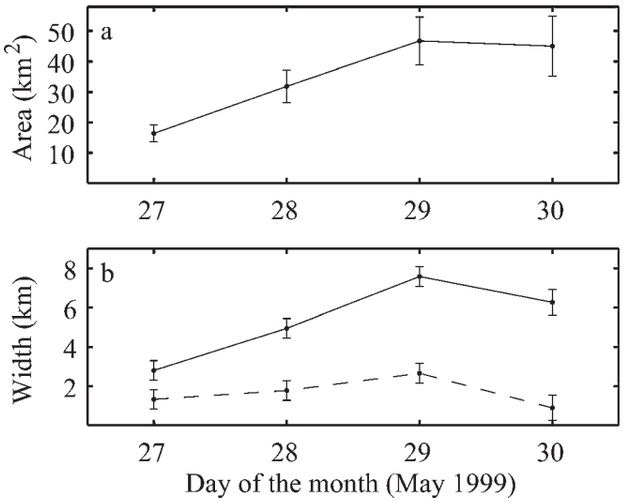

Fig. 5. Plume growth on the basis of the data in Fig. 3. (a) Bulge area. (b) Bulge width (solid line) and average coastal current width (dashed line). Error bars are ±0.5 km, on the basis of the nominal SeaWIFS sensor resolution of 1 km.

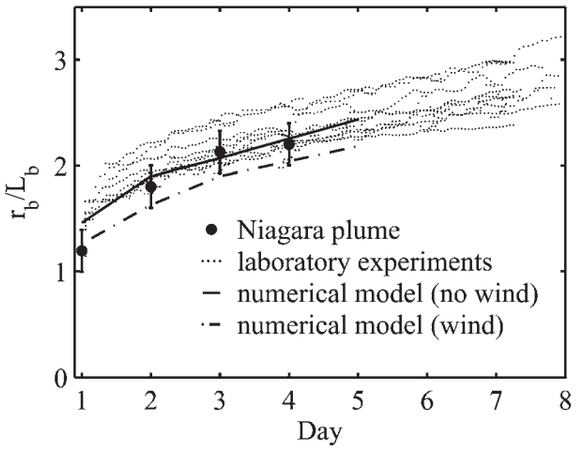

Fig. 6. Comparison of satellite data from the Niagara River plume to laboratory and numerical model studies. The laboratory data are from Horner-Devine et al. (2006), and include 13 experiments spanning a large range of Rossby and Froude numbers. The numerical data were obtained using the same model (ECOM3D) as Fong and Geyer (2002) with inflow parameters set to those of the to the Niagara River during the period 27 to 30 May 1999 with and without wind forcing. Error bars for the satellite data are ±0.5 km, on the basis of the nominal SeaWIFS sensor resolution of 1 km.

The area of the bulge increases from approximately 16 km^2 on the first day to 46 km^2 on the third and fourth days (Fig. 5a). Using a linear fit to the area data we calculate that the average growth rate of the bulge during the first 3 d is 15 km^2 d^{-1}. We measure the maximum width of the bulge for each day and compare it with the average width of the coastal current (Fig. 5b). The bulge width increases by a factor of three from the first to the third day. In the same time the coastal current width stays relatively constant.

To compare the results from the Niagara plume to laboratory data, a representative plume radius is determined on the basis of the plume area according to

$$r_b = \left(\frac{A_b}{\pi}\right)^{0.5} \quad (1)$$

where the bulge is assumed to be circular. In laboratory experiments, the radius of the bulge was found to scale with the internal Rossby radius (Avicola and Huq, 2003; Horner-Devine et al. 2006). On the basis of the Niagara plume parameters, L_b = 3.0 km. In Fig. 6 the normalized radius of the bulge, on the basis of the Niagara satellite data, is plotted for comparison with the laboratory data from Horner-Devine et al. (2006). The satellite data agree well with the laboratory data, although the observed radius is slightly lower than the laboratory experiments predict.

The observed bulge radius is also compared with output from a simple numerical model, estuarine coastal ocean model (ECOM 3D; Blumberg and Mellor 1987). The model configuration is nearly identical to the experiments described in Fong and Geyer (2002), except that the width of the river mouth, river discharge, and temperature anomaly are chosen to approximate the Niagara River parameters during the period under consideration. The model domain is rectangular, with a flat bottom and a vertical wall, and the river inflow consists of warm water discharged uniformly from near-surface grid cells along the vertical wall. The reader is referred to Fong and Geyer (2002) for a more detailed description of the model. Two cases are considered for comparison with the satellite data. In the first, the daily average alongshore wind recorded at St. Catherines airport (Fig. 2b) is used. In the second, the wind is turned off to evaluate the relative effect of the wind on the growth of the plume. Three additional model runs with constant alongshore winds of 3, 5, and 7.5 m s^{-1} were also carried out. The latter runs were used to estimate the threshold wind speed above which unsteady plume dynamics are no longer significant. The results of these runs will be referred to in the discussion section to estimate the frequency of occurrence of the unsteady bulge in the Niagara River plume.

As with the satellite and laboratory data, r_b was calculated on the basis of the surface area of the bulge according to Eq. 1. The normalized radius is plotted for comparison with the satellite data in Fig. 6 for the wind and no-wind cases. The radii predicted by the model with and without wind are both consistent with the radius computed from the satellite data. Differences between the model predictions and satellite data are likely due to the fact that the temperature anomaly is not known exactly and that the model configuration is a simplification of the actual plume. The observed bulge growth rate is also compared with the laboratory and model data. The radius of the bulge in the laboratory experiments increases according to

$$\frac{r_b}{L_b} \sim \left(\frac{t}{T}\right)^n \quad (2)$$

where t is the time after the initiation of the plume, T is the rotation period, and n is an exponent describing the growth rate. In the case of the satellite and numerical model data,

t/T is the equivalent of 1 d. For data from the present study, $n = 0.46 \pm 0.29$. In the experiments of both Avicola and Huq (2003) and Horner-Devine et al. (2006) this exponent was found to be approximately $n = 0.4$. The exponent computed from the numerical model output with wind is $n = 0.34 \pm 0.04$. Thus the growth rate of the observed plume from the Niagara discharge is in agreement with both the laboratory and the numerical model experiments within the error of the measurements.

It should be noted that the initial conditions for the Niagara plume and the laboratory and numerical model experiments are likely to have been quite different. The experimental studies are initiated when the source of buoyant water from the river is turned on. In the Niagara, however, the river discharges are continuous; day one of the observations does not correspond to the initiation of the plume and buoyant plume water must have been present in the vicinity of the river mouth before day one. Nonetheless, it is clear from Fig. 3a that the plume was limited to a region very close to the shoreline at the beginning of the study. This is consistent with the period of persistent $\sim$5 m s^{-1} downwelling winds that preceded the study.

Comparison of the bulge radii computed from the wind and no-wind model runs indicates that, although the wind does modify the plume size slightly, it is not responsible for the observed bulge growth (Fig. 6). The alongshore wind decreases the bulge radius by approximately 11%; however, the decrease is similar on each day. The computed growth rate is $n = 0.31 \pm 0.06$ for the no-wind case, compared with $n = 0.34 \pm 0.04$ for the wind case. This result is not surprising, as the wind is relatively weak during the study period. The role of the wind will be discussed further in the following section.

Discussion

The Niagara River plume demonstrates bulge growth in the absence of strong wind forcing or variable river discharge. The observed bulge growth agrees well with laboratory and numerical model results, in which only the plume buoyancy, the rotation of the earth, and an alongshore current are included. This agreement suggests that the observed growth is also the result of simple plume dynamics. This is the first field evidence supporting the theory of unsteady bulge growth in river plumes suggested by the analytical work of Nof and Pichevin (2001) and by laboratory and numerical models.

During the period from 27 to 29 May we calculate that the area of the bulge increases at a rate of 15 km^2 day^{-1}. In their field study, Masse and Murthy (1992) show vertical density profiles for the bulge area of the plume with an average interface depth of approximately 12 m during a period when the river discharge was similar to this study period. This plume depth is consistent with the scaling estimate presented in the methods section. On the basis of this depth and the area rate of change above, the volume rate of change of the bulge is approximately 2000 m^3 s^{-1}.This is greater than one-third of the river discharge, implying that less than two-thirds of the discharge is transported away from the mouth in the coastal current. The accumulation of water in the bulge implies that waterborne sediments, contaminants, nutrients, and microorganisms may have longer residence times in the vicinity of the river mouth than if the plume were assumed to be steady.

Images of the Niagara River on other days show plume bulges of a similar scale to those described in this paper, but not significantly larger. This implies that the bulge growth is ultimately arrested, presumably by wind or an alongshore ambient current. A strong easterly wind will generate an upwelling flow and force the plume to mix offshore (Fong and Geyer 2001). A strong westerly wind, on the other hand, will reduce the size of the bulge by means of onshore transport and downwelling (Chao 1988). Alternatively, Fong and Geyer (2002) show that an ambient current in the same direction as the coastal current limits the size of the bulge. Masse and Murthy (1992) report that Lake Ontario often has a counterclockwise 8 cm s^{-1} current near the shore. It is likely that this current limits the size of the bulge, whereas winds periodically remove it.

Whitney and Garvine (2005) quantify the influence of alongshore winds on coastal river plumes in terms of a wind strength index, which is the ratio of velocity scales representative of the wind and buoyancy forcing,

$$W_s = \frac{u_{wind}}{u_{dis}} \tag{3}$$

where $u_{dis} = K^{-1}\,(2g'_r Qf)^{1/4}$ and $u_{wind} = (\rho_{air} C_{10})^{1/2}\,(\rho C_{Da})^{-1/2} U$. Here, K is the Kelvin number, which is the ratio of the plume width to the internal Rossby radius, g'_r is the reduced gravity on the basis of the density difference between the river and receiving waters, C_{10} and C_{Da} are surface and bottom drag coefficients, respectively, and U is the wind speed. u_{dis} and u_{wind} represent plume velocities due to buoyancy and wind, respectively. A value of $W_s > 1$ indicates that wind exerts a dominant influence on the dynamics of the plume. On the basis of typical Niagara River plume parameters, and assuming a value of $K = 2$, $u_{dis} = 0.15$ m s^{-1}. Following Whitney and Garvine (2005), $u_{wind} \simeq 2.65 \times 10^{-2} U$. Combining these values for the discharge and wind velocity scales, W_s exceeds 1 when the wind speed $U > 5.7$ m s^{-1}. To test this scaling with the Niagara plume bulge, we carried out model runs with alongshore winds in the downwelling direction of 3, 5, and 7.5 m s^{-1}. The 3 m s^{-1} wind increased the alongshore flux of river water by approximately 5% relative to the no-wind case, whereas the 5 and 7.5 m s^{-1} cases increased it by 47% and 80%, respectively. Thus, the bulge growth, which is inversely related to the alongshore transport, is significantly decreased for winds greater than 5 m s^{-1}. These trends are consistent with the criteria proposed by Whitney and Garvine (2005) and we will use their criteria for the remainder of the analysis.

The average alongshore wind speed during the study period was 3.5 m s^{-1}, consistent with the result that winds did not play a dominant role in the plume dynamics. Analysis of the wind record for the 1999 calendar year shows that the daily average wind only exceeded 5.7 m s^{-1} on 15 d, or less than 5% of the year. This suggests that the dynamics observed during the study period may be relatively common. A more accurate estimate of the frequency of occurrence of the retentive bulge feature in the plume is complicated, however. Although the discharge is relatively constant

throughout the year (Masse and Murthy 1990), the density anomaly depends on the differential heating of Lakes Erie and Ontario, which varies seasonally.

A large coring study of Lake Ontario was conducted in the late 1960s as part of an assessment of the effect of the river on the distribution of contaminants in the lake (Thomas 1983). The study concludes that the Niagara River is the primary source of contaminants such as PCBs and Mirex to lake sediments. The measured distribution of PCBs in lake sediments indicates that contaminants introduced to the lake from the river take two primary paths (Thomas 1983, see Fig. 5). The first hugs the southern shore of the lake, presumably in the coastal current. The second travels north and west, accumulating 10–15 km offshore of the river mouth. This later path is roughly perpendicular to the dominant shore-parallel currents that exist in the absence of the plume. The observation that the Niagara plume sometimes forms a retentive bulge that extends offshore in the vicinity of the river mouth may help to explain the observed distribution of contaminated sediment. Although the distribution is certainly the result of several transport processes, the bulge circulation provides a mechanism for the deposition of fine sediment offshore of the river mouth that would not exist in the absence of the plume.

The Niagara River is a good laboratory for studying river plumes because clear images are available, alongshore currents are weak, and the river discharge is approximately perpendicular to the coast. Many other rivers share similar characteristics, however, and so it is very likely that this phenomenon is more general. Furthermore, bulge formation has been documented on some occasions in rivers for which smaller inflow angles, ambient currents, or shallow slopes typically suppress large bulge growth. Although these external forces mediate bulge growth, it seems likely that the mechanism that limits alongshore transport in the Niagara plume also influences transport in these other plumes.

References

Atkinson, J. F., G. Lin, and M. Joshi. 1994. Physical model of Niagara River Discharge. J. Great Lakes Res. **19:** 83–95.

Avicola, G., and P. Huq. 2003. The characteristics of the recirculating bulge region in coastal buoyant outflows. J. Mar. Res. **61:** 435–463.

Blumberg, A. F., and G. L. Mellor. 1987. A description of a three-dimensional coastal ocean circulation model, p. 1–16. *In* N. Heaps [ed.], Three-dimensional coastal ocean models. AGU.

Chant, R., and others. 2008. Bulge formation of a buoyant river outflow. J. Geophys. Res. **113:** C01017, doi:10.1029/2007JC004100.

Chao, S-Y. 1988. Wind-driven motion of estuarine plumes. J. Phys. Oceanogr. **18:** 1144–1166.

de Boer, G. J., J. D. Pietrzak, and J. C. Winterwerp. 2008. SST observations of upwelling induced by tidal straining in the Rhine ROFI. Cont. Shelf Res. doi:10.1016/j.csr.2007.06.011.

Fong, D. A., and W. R. Geyer. 2001. The response of a river plume during an upwelling favorable wind event. J. Geophys. Res. **106:** 1067–1084.

———, and ———. 2002. The alongshore transport of fresh water in a surfacetrapped river plume. J. Phys. Oceanogr. **32:** 957–972.

Garvine, R. W. 1987. Estuary plumes and fronts in shelf waters: a layer model. J. Phys. Oceanogr. **17:** 1877–1896.

———. 2001. The impact of model configuration in studies of buoyant coastal discharge. J. Mar. Res. **59:** 193–225.

Geyer, R. W., P. Hill, T. Milligan, and P. Traykovski. 2000. The structure of the Eel River plume during floods. Cont. Shelf Res. **20:** 2067–2093.

Harper, A. L. W., and N. S. Kemp. 1976. Sedimentation rates and a sediment buget for Lake Ontario. J. Great Lakes Res. **2:** 324–340. 3

Hickey, B. M., L. J. Peitrafesa, D. A. Jay, and W. C. Boicourt. 1998. The Columbia River plume study: subtidal variability in the velocity and salinity field. J. Geophys. Res. **103:** 10339–10368.

Horner-Devine, A. R. 2008. The bulge circulation in the Columbia River plume. Cont. Shelf Res. doi:10.1016/j.csr.2007.12.012.

———, D. A. Fong, S. G. Monismith, and T. Maxworthy. 2006. Laboratory experiments simulating a coastal river inflow. J. Fluid Mech. **555:** 203–232.

Lanoix, F. 1974. Projet Alboran. Etude hydrologique et dynamique de la mer dAlboran. Rapp. Tech. OTAN **66:** 39–50.

Lentz, S. J., and K. R. Helfrich. 2002. Buoyant gravity currents along a sloping bottom in a rotating fluid. J. Fluid Mech. **464:** 251–278.

Masse, A. K., and C. R. Murthy. 1990. Observations of the Niagra River thermal plume Lake Ontario North America. J. Geophys. Res. **95:** 16097–16109.

———, and ———. 1992. Analysis of the Niagra River Plume. J. Geophys. Res. **97:** 2403–2420.

Mertes, L. A. K., and J. A. Warrick. 2001. Measuring flood output from 110 coastal watersheds in California with field measurements and SeaWiFS. Geology **29:** 659–662.

Murthy, C. R. 1996. Particle pathways of Niagara River water in Lake Ontario affecting bottom sediment concentration. Hydrobiologia **322:** 109–116.

Nof, D., and T. Pichevin. 2001. The ballooning of outflows. J. Phys. Oceanogr. **31:** 3045–3058.

Pichevin, T., and D. Nof. 1997. The momentum imbalance paradox. Tellus **48:** 298–319.

Salisbury, J. E., J. W. Campbell, E. Linder, L. D. Meeker, F. E. Mller-Karger, and C. J. Vrsmarty. 2004. On the seasonal correlation of surface particle fields with wind stress and Mississippi discharge in the northern Gulf of Mexico. Deep-Sea Res. II **51:** 1187–1203.

Thomas, A. C., and R. A. Weatherbee. 2006. Satellite-measured temporal variability of the Columbia River plume. Remote Sens. Environ. **100:** 167–178.

Thomas, R. L. 1983. Lake Ontario sediments as indicators of the Niagara River as a primary source of contaminants. J. Great Lakes Res. **9:** 118–124.

U.S. EPA and NYSDEC. 1998. Reduction of toxics loadings to the Niagara River from hazardous waste sites in the United States: November 1998. Technical Report of the U.S. Environmental Protection Agency Region 2.

Warrick, J. A., and D. A. Fong. 2004. Dispersal scaling from the worlds rivers. Geophys. Res. Lett. **31**, doi:10.1029/2003GL019114.

Whitney, M. M., and R. W. Garvine. 2005. Wind influence on a coastal buoyant outflow. J. Geophys. Res. **110:** C03014, doi:10.1029/2003JC002261.

Yankovsky, A. E., and D. C. Chapman. 1997. A simple theory for the fate of buoyant coastal discharges. J. Phys. Oceanogr. **27:** 1386–1401.

Received: 28 July 2007
Accepted: 21 April 2008
Amended: 16 June 2008